VELOCITY FLOW PROFILES OVER SMOOTH BED IN OPEN CHANNELS

Abubaker M. Abusbeaa, and Salaheddin N. Shmela

Civil Engineering Department, Faculty of Engineering,
Al-Fateh University, Tripoli, Libya

الملخص

الدفق خلال معظم القنوات الطبيعية والمنشآت الهيدروليكية هو من النوع المضطرب. إن متوسط توزيع السرعة في المستوى المتعامد على السطح لقاع القناة ذو أهميه كبيرة للمهندسين وذلك في حالات تحليل الدفق ثنائي الأبعاد. عدد من الأبحاث النظرية والتجريبية تناولت إيجاد التوزيع الرأسي للسرعات في طبقات الإجهاد القصي المضطرب على الأسطح الخشنة والملساء. إن هذه الدراسة تستقصي متوسط توزيع السرعة لدفق منتظم مضطرب على الأسطح الملساء لقيعان القنوات المفتوحة وتقارنها ببعض النماذج النظرية المتاحة ونتائج التجارب قد أظهرت أن توزيع السرعة رأسيا من مستوى قاع القناة يمكن تقديره ببعض النماذج شريطة أن بعض المعاملات تقرب نسبيا وإن حالات الدفق المختلفة يمكن تحديدها. إن الاعتقاد السائدة بأن بعض هذه النماذج لها خاصية العمومية ويمكن تطبيقها على اغلب حالات الدفق ليست صحيحة كليا.

ABSTRACT

The study investigates mean velocity distribution of uniform turbulent flows over smooth channel beds and compares these profiles with certain available models. Experiment results show that velocity profiles can be estimated by certain theoretical models provided that some parameters are approximated and flow conditions are defined. The theory that some models are universal and can be used for all types of flows in the general sense can not stand.

KEYWORDS: Open channel; Velocity profiles; Velocity distribution; Velocity components; Shear velocity; Smooth beds.

INTRODUCTION

Real fluids are usually classified into two categories of laminar flow and turbulent flow. Almost all geophysical (natural) flows are turbulent which in nature occur in rivers, lakes, estuaries and oceans. Almost all the flows in man-made hydraulic structures, such as spillways, weirs, convergence channel, irrigation networks, water supplies, sewers, harbours and fluvial works are turbulent.

Velocity profiles resulting from turbulent flow over plane structures are of great interest to the engineer. It is the mean (time averaged) velocity distribution near the planes which governs shear stress on the bottom. Bottom roughness, bulk fluid velocity and fluid properties such as viscosity and density are the primary factors which regulate the resultant velocity variation.

The many studies of open-channel flows indicate that, like boundary layers and closed channel flows, open channel flows also consist of two regions, a near wall region, and an outer region near the free surface. For two-dimensional open channel flows, the near-wall region is controlled by the inner variables, namely the kinematic

viscosity, υ, and the friction velocity, U_*. Figure (1) shows a sub-division of the open-channel field. The features of the near-wall region are virtually the same as those observed in the boundary layers and closed-channel flows, as pointed out by Coles (1978). On the other hand, the outer region is controlled by the flow depth, h, and maximum main stream velocity, Umax.

The flow in natural streams and in rectangular channels of finite aspect ratio, b/h (in which b = width; h = the depth of flow), is distorted by lateral diffusion of vorticity from the channel sidewalls and transverse circulations generated by secondary currents. The resulting velocity distribution can then be closely predicts, if it can be predicted at all, only by means of numerical integration of the three dimensional equations governing the fluid motion, Deardorff (1970) and others. There are, however, practical situations involving channels and conduits where the sidewall effect and secondary currents, though present, are too weak to cause pronounced distortion, and in these situations the involved computational procedures used in the studies previously mentioned can be replaced by simpler methods. The theoretical investigations of Prandtl (1933) and Von Karman (1930) on flow through pipes, and experimental studies of Nikuradse (1933) have led to rational formulas for velocity distribution and hydraulic resistance for turbulent flows over flat plates and circular pipes. These formulas have been extended to open channel flows. Although there are some general similarities between the pipe flow and the open-channels flow, certain factors such as the presence of a free surface, three dimensional nature of flow due to non-circular cross-section of the channel, and non-uniform distribution of sheer along the wetted perimeter, distinguish open-channel flow from pipe flow

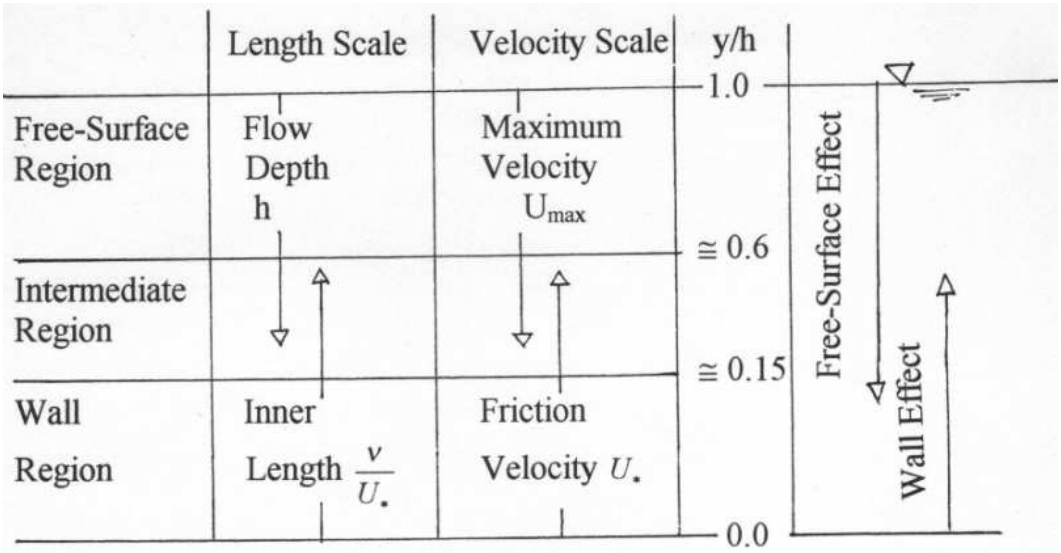

Figure 1: Sub-division of the open-channel field, Nezu and Nakagawa (1993)

THEORY OF TWO-DIMENSIONAL VELOCITY

As shown in Figure (2), U, V, and W denote the components of mean velocity; u, v, and w denote the fluctuations and u', v', and w' denote the r.m.s. values, i.e., turbulent intensities, in the x-direction(stream wise with the origin at the channel entrance), y-direction (vertical wise with the origin at the channel bed), and z-direction (span wise with the origin at the channel center), respectively. The continuity and

Reynolds equations derived from the Navier-Stokes equations, for steady, two-dimensional (2-D) open-channel flows are as follows; Nezu and Nakagawa (1993):

$$\frac{\partial U}{\partial x} + \frac{\partial V}{\partial y} = 0 \tag{1}$$

$$U\frac{\partial U}{\partial X} + V\frac{\partial U}{\partial y} = g\sin\theta - \frac{\partial}{\partial x}\left(\frac{P}{\rho}\right) + \frac{\partial}{\partial x}(-\overline{u^2}) + \frac{\partial}{\partial y}(-\overline{uv}) + \nu\nabla^2 U \tag{2}$$

$$U\frac{\partial V}{\partial x} + V\frac{\partial V}{\partial y} = -g\sin\theta - \frac{\partial}{\partial y}\left(\frac{P}{\rho}\right) + \frac{\partial}{\partial x}(-\overline{uv}) + \frac{\partial}{\partial y}(-\overline{v^2}) + \nu\nabla^2 V \tag{3}$$

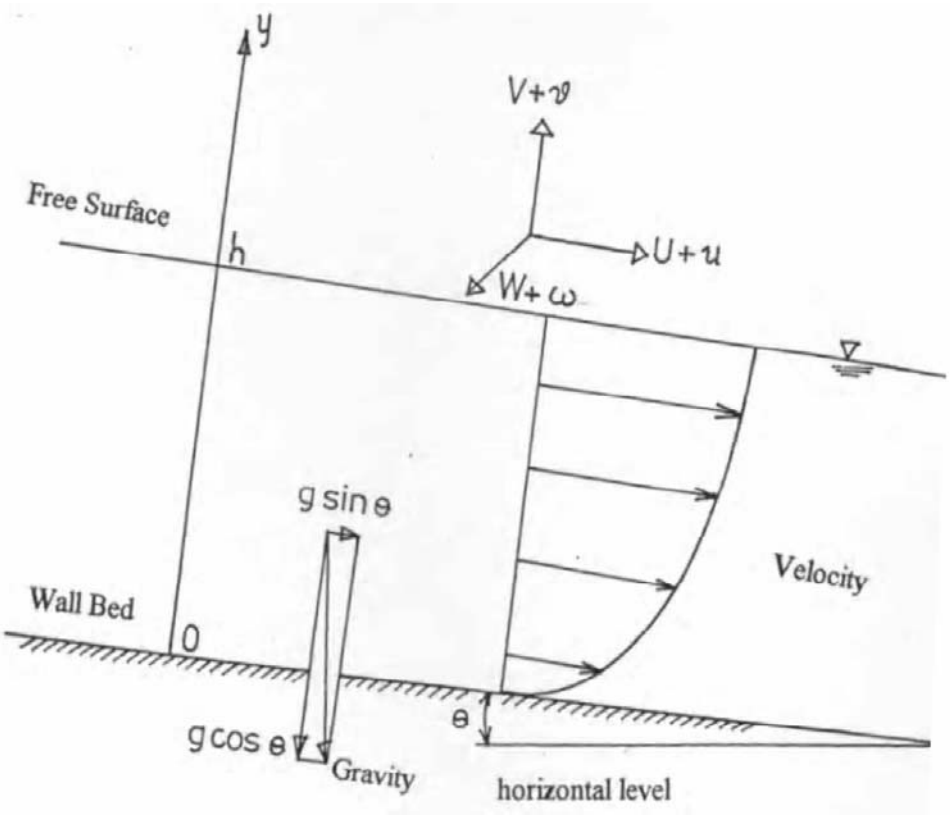

Figure 2: Coordinate system in open-channel flows

where P is the mean pressure, ρ the fluid density, g the gravitational acceleration, υ kinematic viscosity, and θ the angle of channel slope to the horizontal axis. The symbol ∇^2 denotes the Laplacian operator. In uniform open-channel flow, for which $V = 0$ and $\frac{\partial}{\partial x} = 0$, equation (3) can be integrated in the y-directional as follows:

$$\frac{P}{\rho} = (h - y)g\cos\theta + (v_s^{'2} - v^{'2}) \tag{4}$$

where h is the flow depth. The quantity of $v_s^{'}$ is the magnitude of the vertical fluctuation at the water surface; it reduces to zero due to the existence of the free surface (free of shear, free of turbulence). The first term on the right hand side of Equation (4) is the hydrostatic pressure distribution; the second term indicates the contribution of

turbulence to the mean pressure $\frac{p}{\rho}$. A combination of Equations (2) and (4), after integration, leads to

$$\frac{\tau}{\rho} \equiv -\overline{uv} + \nu\frac{\partial U}{\partial y} = U_*^2\left(1 - \frac{y}{h}\right) \tag{5}$$

$$\frac{\tau_b}{\rho} \equiv U_*^2 = gh(\sin\theta - \cos\theta\frac{dh}{dx}) \equiv ghI_e \tag{6}$$

where U_* is the friction velocity and I_e is the energy gradient, i.e. $I_e = \sin\theta - \cos\theta\frac{dh}{dx}$ Equation (5) indicates that the total shear stress τ varies linearly from the value τ_b at the bed ($y = 0$) to zero at the free surface ($y = h$).

FLOW FIELD IN OPEN CHANNEL

In bounded shear flow, fully developed turbulent shear layers consist of inner and outer regions Cebeci and Smith (1979); Coleman and Alonso (1983). The upper limit of the boundary influence, on the top of the boundary layer, is at the time location of the maximum velocity displayed by the local velocity profile.

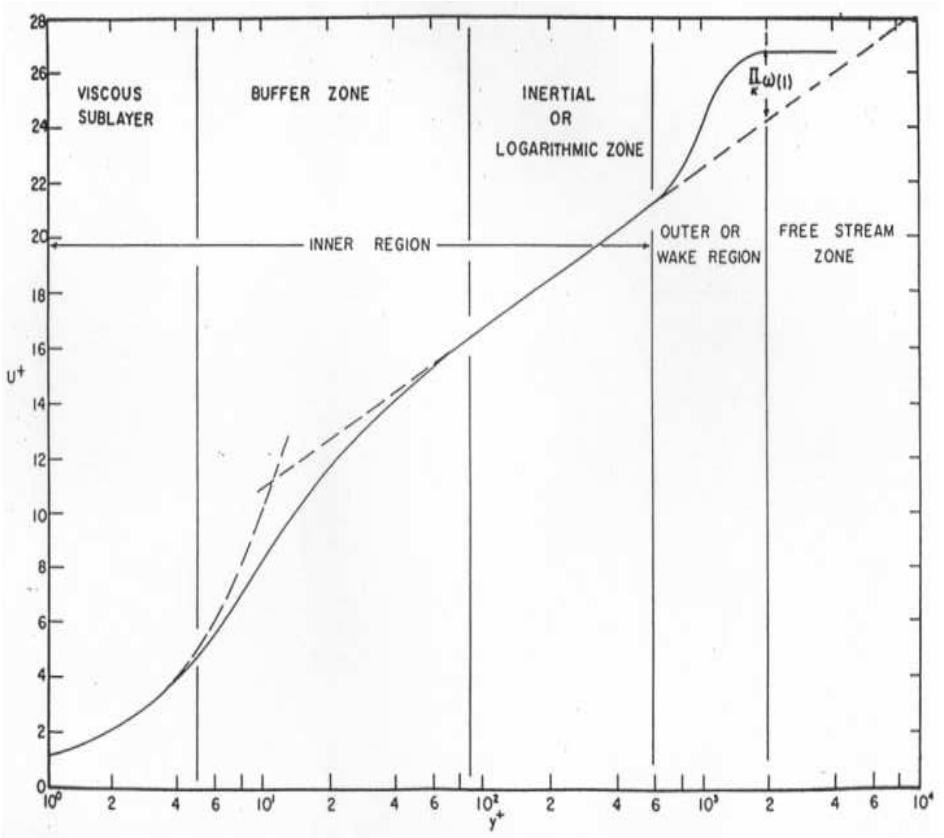

Figure 3: The zones and regions of bounded shear flow, Coleman and Alonso (1983)

Within the boundary layer thickness, the bounded shear flow can be divided as shown in Figure (3) into the outer, or wake region, and an inner or wall region. Above the boundary layer top is the free stream zone. Figure (3) is a non-dimensional plot in which the local velocity U, at a distance Y from the boundary, is normalized by the

boundary shear velocity $U_* = \sqrt{\tau/\rho}$ to give the similitude term $U^+ = \frac{U}{U_*}$, and Y is normalized with viscous length $\frac{\upsilon}{U_*}$ to give the dimensionless Y- coordinate $Y^+ = \frac{U_* y}{\upsilon}$.

THE OUTER REGION (CORE LAYER)

The flow in this region is influenced by the constrain of the entire periphery of the channel geometry in case of flow through channels. This layer is controlled by the flow depth and the maximum velocity, Umax, and it extends up to the free surface of flows through open-channels. The distinction between the turbulent flow in the inner region and that in the outer region stems from the fact that the turbulence in the inner region is directly influenced by the wall, whereas it is not in the outer region, through there is still some interaction between the two regions.

FRICTION VELOCITY

Detailed investigation of turbulent flow in open-channel flow requires accurate evaluation of the friction velocity U∗. This parameter is the most fundamental velocity scale with which to normalize mean velocity and turbulence. The friction velocity can be determined by various methods such as using Reynolds stress distribution *uv* (y), in conjunction with equation (5).

SMOOTH BED MEAN VELOCITY PROFILES

In the two-dimensional analysis of fluid flows, the mean velocity distribution in the plane perpendicular to the solid boundary is of great interest to engineers. A number of analytical investigators (Willis 1972, Song and Yang 1979, Still 1982, Coleman and Alanso 1983, Vendula and Achanta 1985; Willis 1985) and experimental investigators (Kamphius 1974, Bayazit 1976, Zippe and Graf 1983, Sarma et al. 1983, Kirkgöz 1989, Ferro and Baiamonte 1994, Song et al. 1994, Xinyu et al. 1995) have sought to determine the vertical distribution of velocities for turbulence shear layers on both smooth and rough surfaces.

THE LAW OF THE WALL

$$U^+ = Y^+ \quad \text{for} \quad Y^+ << B \quad \text{(viscous sub layer formula)} \tag{7}$$

$$U^+ = \frac{1}{\kappa}\ln(Y^+) + A \quad \text{for} \quad B \leq Y^+ \leq Re_* \quad \text{(log-law formula)} \tag{8}$$

where κ is the von-Karman constant ($\kappa \cong 0.400 - 0.412$) and A is a constant of integration ($A = 4.9 - 7.0$) and B is a damping factor ($B \cong 26$)

$$Re_* = \frac{U_* h}{\upsilon}$$

THE VELOCITY DEFECT LAW

$$U^+ = \frac{1}{\kappa}\ln(y^+) + A + \omega(y/h) \tag{9}$$

for the outer region velocity distribution. $\omega(y/h)$ is a wake function given empirically by Coles (1956)

$$\omega(y/h) = 2\frac{\Pi}{\kappa}\sin^2\left(\frac{\pi y}{2h}\right) \quad (10)$$

where Π is Coles' wake strength parameter.
Equation (9) & (10) yield:

$$U^+_{max} - U^+ = -\frac{1}{\kappa}\ln\left(y/h\right) + \frac{2\Pi}{\kappa}\cos^2\left(\frac{\pi y}{2h}\right) \quad (11)$$

In which

$$U^+_{max} = \frac{U_{max}}{U_*}$$

Since the velocity distribution is determined over the whole flow depth by the log-wake law, the bulk mean velocity U_m and friction law are obtained as:

$$\sqrt{2/C_f} = \frac{1}{\kappa}\ln\left(Re\sqrt{2/C_f}\right) + \left(A - \frac{1}{\kappa}\right) + \frac{\pi}{\kappa} \quad (12)$$

$C_f = 2\left(\frac{U_*}{U_m}\right)^2$ is the friction coefficient, and $Re = \frac{U_m h}{\upsilon}$ is the Reynolds number based on the bulk mean velocity U_m and flow depth h. For smooth bed inner region $\kappa = 0.41$ & $A = 5.29$ Nezu and Rodi (1986).

Coleman and Alonso (1983) gave a multiple-zone model, equation (13), of velocity distribution throughout the complete inner and outer regions of smooth and rough open channel flows provided that $\kappa^+ < 2000$

$$U^+ = \int_0^{y^+} 2/\left\{1 + \left\{1 + [2\kappa(t^+ + \Delta t^+)]^2\left[1 - \exp\left(\frac{-t^+ - \Delta t^+}{26}\right)\right]^2\right\}^{1/2}\right\} dt^+ + \left(\frac{y^+}{\Delta^+}\right)^2\left(1 - \frac{y^+}{\Delta^+}\right) + \left(\frac{2\pi}{\kappa}\right)\left(\frac{y^+}{\Delta^+}\right)^2\left[3 - 2\left(\frac{y^+}{\Delta^+}\right)\right] \quad (13)$$

Where t^+ is a dummy variable and

$\Delta^+ = \Delta\frac{U_*}{\upsilon}$ = dimensionless boundary layer thickness $\cong$ h.

If a standard value of κ such as 0.41 is used, the model requires independent prediction of the parameters Δ^+, k_s^+, and π in order to have practical use.

$$\Delta t^+ = 0.9\left[(k_s^+)^{1/2} - k_s^+\exp\left(\frac{-k_s^+}{6}\right)\right] \quad (14)$$

k_s^+ = *dimensionless equivalent sand roughness*

EXPERIMENTAL SETUP AND PROCEDURE

The experiments were performed in 5.5 m long, 0.25 x 0.25 m cross section glass walled flume with an adjustable bed slope, see Figure (4). The channel bed was used directly for the smooth bed experiments. For all tests, water at room temperature was the fluid media and the flow was steady uniform. All flow velocities were measured at mid-verticals of the flow cross-section, where the flow supposed to be least affected by three dimensionalities. Velocity components were measured by the Laser-Doppler Anemometry (LDA) system. Two flow regimes were utilized, the normal (uniform) flow regime for which the flow surface draws down in the downstream direction, and

the back water flow regime where the flow surface was kept horizontal by some kind of weir located at the outlet end of the flume. The aspect ratio (i.e., the width-to-depth ratio) of flow varied between 2.27 and 16.13.

Some details of the tests are summarized in Table (1) , in which q is the unit discharge of flow; h is the flow depth R_h in the hydraulic radius of the flow cross-section; U_m is the bulk mean velocity of flow; b/h is the flow aspect ratio; $Fr = \left(\frac{U_m}{\sqrt{gh}}\right)$ is the flow Froude numbers; $R_{e_h} = \left(\frac{\Delta h R_h}{\nu}\right)$ is the Reynolds number; $U_*^{(1)}$ is the shear velocity calculated from the energy grade line, $U_*^{(2)}$ is the friction velocity from the measured Reynolds-stress profile; $U_*^{(3)}$ is the shear velocity determined from the log-distribution $U^+ = \frac{1}{\kappa}\ln(y^+) + A$ with $\kappa = 0.40$ and A = 5.5 ; $U_*^{(4)}$ is the shear velocity determined to fit linear velocity distribution in the vicinity of smooth wall (viscons sublayer),

$U^+ = Y^+$

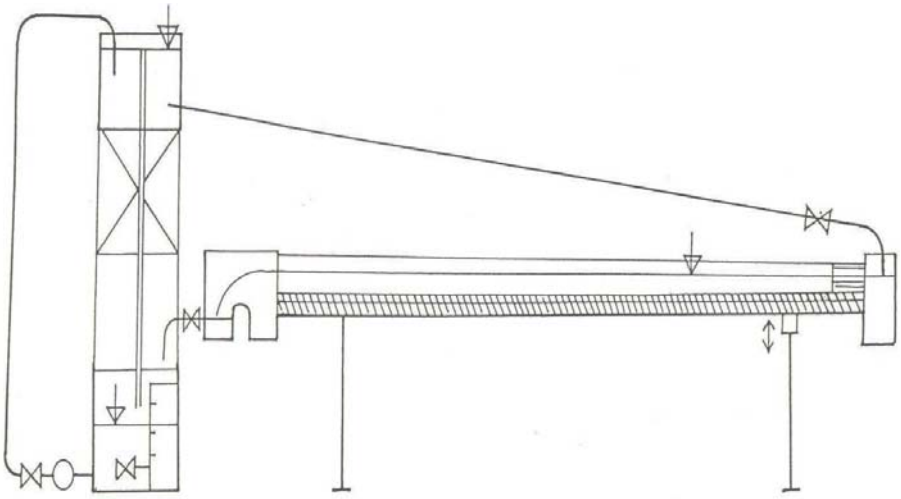

Figure 4: Experimental equipment, schematic diagram

RESULTS AND DISCUSSIONS

The results of the test described in Table (1) are presented in Figures (5) to (10). Figure (5) gives the normalized measured velocity distribution.

DETERMINATION OF SHEAR VELOCITY

The shear velocity has been obtained from the measured Reynolds stress distribution when available, or by using the normalized measured velocity distribution in the viscous-sublayer given in Figure (6). Assuming that the velocity distribution in the vicinity of the smooth wall is linear, and then the shear velocity can be obtained from Equation (7). The calculated values of the shear velocities using Equation (7) are given as $U_*^{(3)}$ in Table (1). These values seem to compare well with those given by other methods. It is clearly seen from Figures (6) and (7) that the viscous sublayer thickness tends to decrease with increasing Reynolds number. It is also seen that the velocity flow, U, keeps almost constant values near the free surface of flow.

Table 1 Summary of the flow parameters for experiments

Flow Reg. (1)	Bed Type (2)	Run No. (3)	Channel Bed Slope (4)	q (l/s/m) (5)	h (mm) (6)	R_h (m) (7)	U_m (m/s) (8)	b/h (9)	Fr (10)	Re_h (11)	$U_*^{(1)}$ (cm/s) (12)	$U_*^{(2)}$ (cm/s) (13)	$U_*^{(3)}$ (cm/s) (14)	$U_*^{(4)}$ (cm/s) (15)	Π (17)
	Smooth	N1			40.00	0.030	0.405	6.25	0.65	49100	2.18	2.20	2.19		0.30
	Rough 1	A1	0.00123		42.50	0.032	0.381	5.88	0.59	48300	2.70	2.80			0.30
	Rough 2	A2			43.00	0.032	0.377	5.81	0.58	48250	3.28	3.20			0.30
	Rough 3	A3			48.00	0.035	0.338	5.21	0.49	46900	3.67	3.70			0.10
	Smooth	N2			25.00	0.021	0.648	10.00	1.31	53900	3.75	3.50	3.45		0.30
	Rough 1	B1		16.20	31.40	0.025	0.516	7.96	0.93	51800	4.20	4.00			0.10
	Rough 2	B2			36.20	0.028	0.448	6.91	0.75	50350	4.40	4.10			0.10
	Rough 3	B3	0.00615		39.80	0.030	0.407	6.28	0.65	49200	4.60	4.45			0.10
	Smooth	BW1			76.00	0.047	0.213	3.29	0.25	40300		1.10	1.16		0.55
	Rough 1	C1			70.00	0.045	0.231	3.57	0.28	41500		1.70			0.40
	Rough 2	C2			65.00	0.043	0.249	3.85	0.31	42600		2.15			0.30
	Rough 3	C3			60.50	0.041	0.268	4.13	0.35	43950		2.95			0.10
		N3		19.10	42.50	0.032	0.449	5.88	0.81	57520				2.25	
		N4		5.65	23.50	0.020	0.240	10.64	0.55	19234				1.45	
		N5		2.70	15.50	0.014	0.174	16.13	0.47	9608				1.13	
		BW2		19.04	110.00	0.059	0.173	2.27	0.23	40447				0.90	
	Smooth	BW3	0.0000	19.10	91.00	0.053	0.210	2.75	0.41	44520				1.05	
		BW4		19.10	74.50	0.047	0.258	3.36	0.38	48193				1.28	
		BW5		19.10	97.60	0.055	0.196	2.56	0.27	42902				0.97	
		BW6		19.10	69.30	0.045	0.276	3.61	0.42	49151				1.38	
		BW7		19.10	51.00	0.036	0.375	4.90	0.63	55346				1.79	

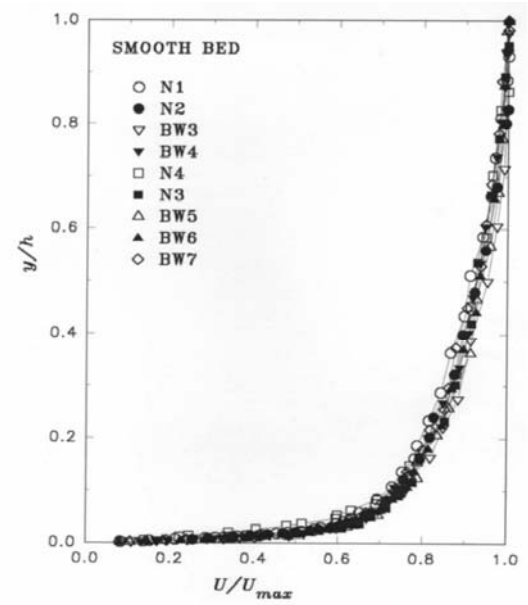

Figure 5: Non-dimensional velocity distributions for smooth bed

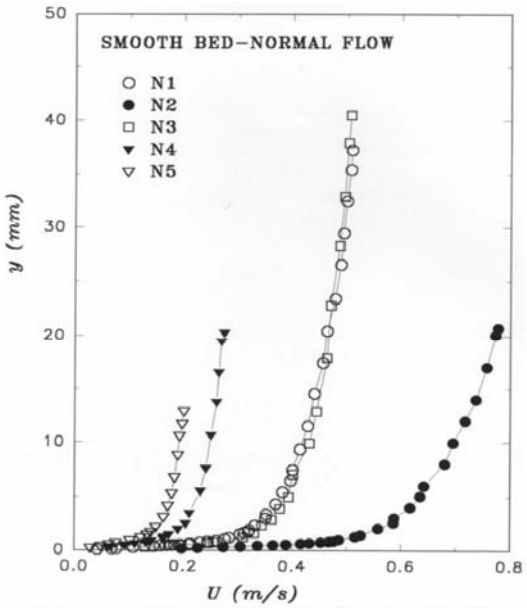

Figure 6: Measured velocity distributions for smooth bed in normal flow regime

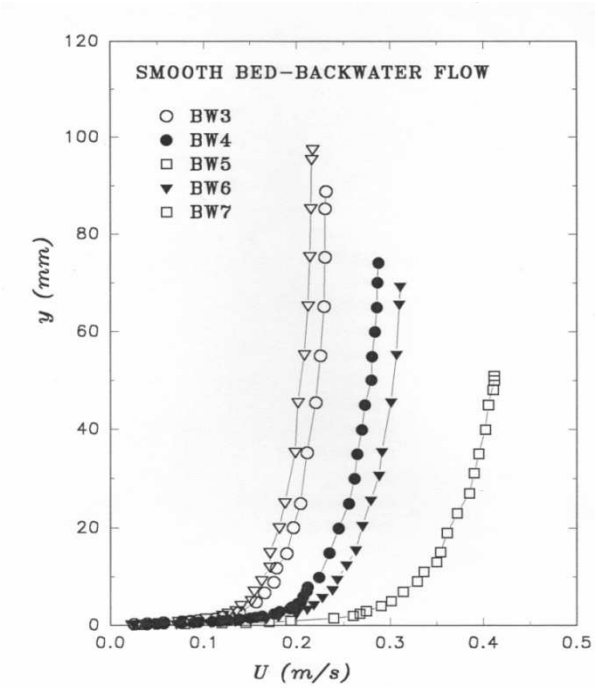

Figure 7: Measured velocity distributions for smooth bed in backwater flow regime

LAW-OF-THE-WALL-DISTRIBUTION

With known values of shear velocities, the law-of-the-wall distributions are calculated and given in Figure (8). The overall data in the turbulent part of the inner region are best represented by Equation (13); Coleman and Alonso (1983) with $\kappa = 0.41$. In the same region the data compares fairly well with equation (8) with different values of κ.

$\kappa = 0.41$ and $A = 5.5$, Kirkgos (1989)

$\kappa = 0.40$ and $A = 6.0$, Xinyu et al. (1995)

For the range of Reynolds number conditions tested, Equation (8) is valid in the range $30 - 50 \leq Y^+ \leq 400 - 600$ see Figure (2). In Figure (8) the limiting values of κ and A are plotted and compared with the measured data which falls somewhere in the middle of these limits. In the lower part of Figures (8) and (9) the velocity distribution seem to compare well with Equation (7) showing the viscous sublayer for $Y^+ \leq 5 - 7$

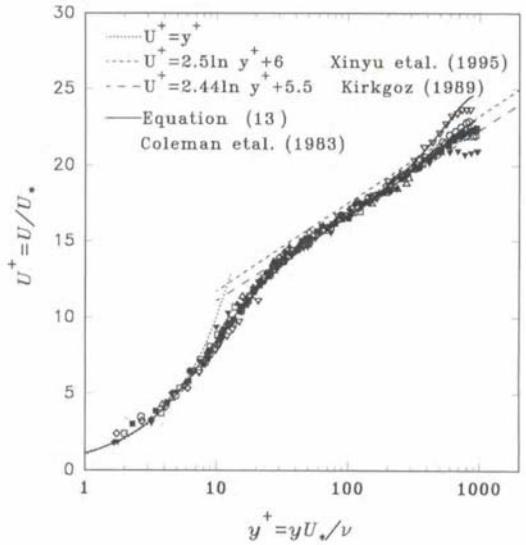

Figure 8: Law of the wall distribution for smooth bed

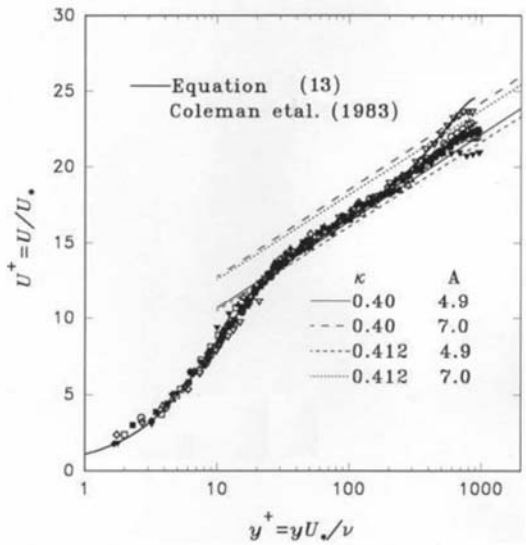

Figure 9: Law of the wall distribution for smooth bed with limiting values of κ and A

VELOCITY-DEFECT DISTRIBUTION

In the outer region of the turbulent boundary layers the velocities are mainly controlled by the turbulent shearing and the velocity distribution can be described, by the velocity-defect law, such as,

$\frac{U_{max} - U}{U_*} = -2.44 \ln (y/h)$, originally given by Prandtle (1933) which was supposed to apply to both smooth and rough walls, and Coles' law given by Equation (11).

The velocity defect distribution of the mean velocities is given in Figure (10), in which the Prandtl Equation and Coles' law are also included. The data points seem to conform reasonably well for $y/h \geq 0.03$.

While the prediction of the velocity defect distribution by the Prandtl Equation is reasonable, Coles' expression, Equation (13), falls completely outside the data points for parameter $\Pi = 0.55$. Zippe et al (1984) argues that the second term in Coles' wake law must have other constant in order to fit the channel data. In supporting their view, Nezu and Rodi (1986) found that the profile parameter π was constant at a value of approximately 0.2, which was considerably smaller than the Coles' values of 0.55. They also reported that the π value found by Steffler et al. (1985) was even lower (varying between 0.08 and 0.15). In Figure (10), Coles' velocity-defect law is drawn of $\kappa = 0.41$ and $\Pi = 0.10$. As may be seen from the Figure, Coles' expression with the fore mentioned values follows the experimental points reasonably well. This leads to the conclusion that in open channel flows, the profile parameter π can be below 0.55 values given by Coles (1956).

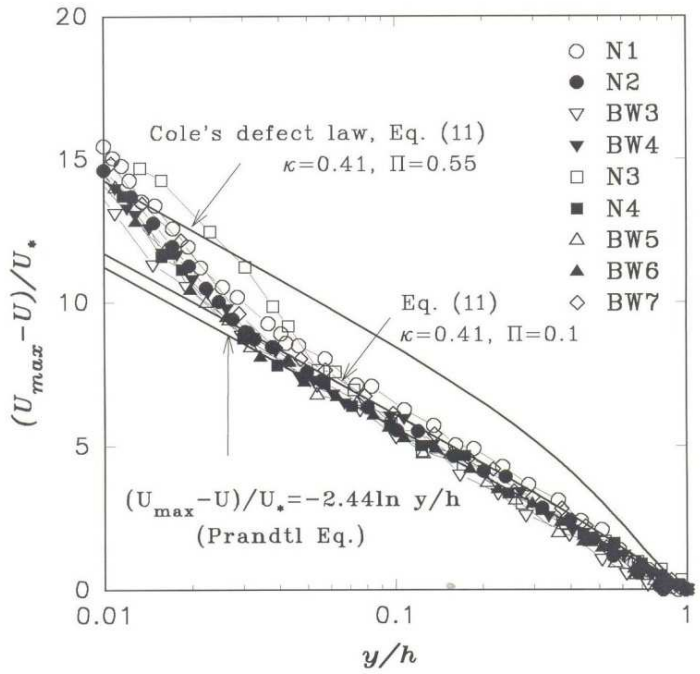

Figure 10: Velocity-defect distributions for smooth bed

CONCLUSIONS

Flow velocities were measured by LDA at mid-vertical of the flow cross-section, where the flow is supposed to be two dimensional. From the presented data, it can be concluded that:

- For any turbulent flow conditions, determination of velocity distribution along the vertical requires an acceptable estimate of the shear velocity, which is not an independent parameter. It depends on other factors; hence it is quite valuable to determine the shear velocity as close as possible to the actual value in order to be able to have a reasonable close distribution to the real case.
- Although von Karman constant, κ, and the constant of integration, A, may have some kind of universal value, it remains well known that each case of flow has its own conditions and properties and it has to be treated within the frame of the dependant parameters and their specific cases. Velocity profiles are extremely sensitive to the κ values and to a less extent to the A constant value.
- Shear velocity of flow can be reasonably estimated from the measured Reynolds stress distribution.
- The distribution of flow velocity can be described by a theoretical model provided that the shear velocity is known. The major data compares well with Coleman and Alonso (1983) model which predicts the velocity profile throughout the complete inner and outer regions of channel-flow.
- The turbulence intensity distribution shows reasonable agreement with distribution calculated by Nezu and Rodi (1985).

REFERENCES

[1] Bayazit, M. (1976). "Free surface flow in a channel for large relative roughness" J. Hydr. Res., 14 (2); 115-126.

[2] Cebeco, T., and Smith, A.M.O. (1974). "Analysis of turbulent boundary layer" Academic Press, New York, N.Y.
[3] Coleman, N.L., and Alonso, C.V. (1983). "Two-dimensional channel flows over rough surfaces." J. Hydr. Engrg., ASCE, 109 (2); 175-188.
[4] Coles, D. (1956). "The law of the wake in the turbulent boundary layer" J. Fluid Mech., 1; 191-226.
[5] Coles, D. (1978). "A model of flow in the viscous sublayer" AFOSR/ Lehigh Univ. Workshop on Coherent Structures of Turbulent Boundary Layer, Lehigh University; 462-474.
[6] Deardorff, J.W. (1970). "A numerical study of three-dimensional turbulent channel flow at large Reynolds numbers." J. Fluid Mech., 1; 453-480.
[7] Ferro, V., and Balamonte, G. (1994). "Flow velocity profiles in gravel-bed rivers" J. Hydr. Engrg., ASCE, 120 (1); 60-79.
[8] Kamphius, J.W. (1974). "Determination of sand roughness for fixed beds." J. Hydr. Res. 12 (2); 193-203.
[9] Kirkgöz, M.S. (1989). "Turbulent velocity profiles for smooth and rough open channel flow." J. Hydr. Engrg., ASCE, 115 (11); 1543-1561.
[10] Nezu, I., and Rodi, W. (1986). "Open-channel flow measurements with a Laser Doppler Amemometer" Hydr. Engrg., ASCE, 112 (5); 335-355.
[11] Nezu, I., and Nakagawa, H. (1993). "Turbulence in Open Channel Flows." IAHR, Monograph.
[12] Nikuradse, J. (1933). "Law of turbulent flow in rough pipes." Translation by NACA, TM 1292, Nov., 1950 (originally published in German).
[13] Prandtl, L. (1933). "Recent results of turbulent research." Translation by NACA, TM 720 (originally published in German).
[14] Sarma, K.V.N., Lakshminarayana, P., and Rao, N.S.L. (1983). "Velocity distribution in smooth rectangular channels." J. Hydr. Engrg., ASCE, 109 (2); 271-289.
[15] Still, B.L. (1982). "New flat plate turbulent velocity profile." J. Hydr. Engrg., ASCE, 108 (1); 1-15.
[16] Song C.S., and Yang, C.T. (1979). "Velocity profiles and maximum stream power" J. Hydr. Engrg., ASCE, 105 (8); 981-998.
[17] Steffler, P.M., Rajaratnam, N., and Peterson, A.W. (1985). "LDA measurements in open-channel." J. Hydr. Engrg., ASCE, 111 (1); 119-130.
[18] Vedula, S., and Achanta, R.R. (1985). "Bed shear from velocity profiles: a new approach." J. Hydr. Engrg., ASCE, 111 (1); 131-143.
[19] Von Karman, T. (1930). "Mechanical similitude and turbulence" Translation by NACA, TM 611 (originally published in German).
[20] Willis, J.C. (1972). "A new mathematical model for the velocity distribution in turbulent shear flow." J. Hyrd. Res. 10 (2); 205-225.
[21] Willis, J.C. (1975). "New bed velocity distribution." J. Hydr. Engrg., ASCE, 111 (5); 741-753.
[22] Xinyu, L., Zenganan, D., and Changzhi, C. (1995). "Turbulent flows in smooth wall open-channels with different slopes." J. Hydr. Res., IAHR, 33 (3); 333-347.
[23] Zippe, H.J., and Graf, W.H. (1983). "Turbulent boundary-layer over permeable and non-permeable rough surfaces." J. Hydr. Res., 21 (1); 51-65.